A remark on limits of triply periodic minimal surfaces of genus 3

Norio Ejiri[*], Shoichi Fujimori,[†] and Toshihiro Shoda[‡]

June 20, 2014

Abstract

In this paper, we consider limits of triply periodic minimal surfaces in $\mathbb{R}^3$. We prove that some important examples of singly or doubly periodic minimal surfaces can be obtained as limits of triply periodic minimal surfaces. Moreover, we give a mathematical proof of the existence of one-parameter family of triply periodic minimal surfaces which is defined in chemistry.

1 Introduction

A minimal surface in $\mathbb{R}^3$ is said to be *periodic* if it is connected and invariant under a group Γ of isometries of $\mathbb{R}^3$ that acts properly discontinuously and freely (see [6]). Γ can be chosen to be a rank three lattice Λ in $\mathbb{R}^3$ (the triply periodic case), a rank two lattice $\Lambda \subset \mathbb{R}^2 \times \{0\}$ generated by two linearly independent translations (the doubly periodic case), or a cyclic group Λ generated by a screw motion symmetry, that is, a rotation around the x_3-axis composed with a non-trivial translation by a vector on the x_3-axis (the singly periodic case). The geometry of a periodic minimal surface in $\mathbb{R}^3$ can usually be described in terms of the geometry of its quotient surface M in the flat three manifold $\mathbb{R}^3/\Lambda$. Hence a triply periodic minimal surface is a minimal surface in a flat torus $\mathbb{T}^3$, a doubly periodic minimal surface is a

[*]Partially supported by JSPS KAKENHI Grant Number 22540103.
[†]Partially supported by JSPS Grant-in-Aid for Young Scientists (B) 25800047.
[‡]Partially supported by JSPS Grant-in-Aid for Young Scientists (B) 24740047.

minimal surface in $\mathbb{T}^2 \times \mathbb{R}$ where $\mathbb{T}^2$ is a flat two torus, and a singly periodic minimal surface is a minimal surface in $S^1 \times \mathbb{R}^2$.

Many of beautiful examples of minimal surfaces in $\mathbb{R}^3$ have this periodic behavior, for example, the helicoid, Scherk's surface, and Schwarz' surface. Also, triply periodic minimal surfaces are related to natural phenomena and many one-parameter families of triply periodic minimal surfaces have been studied in physics, chemistry, and crystallography. Recently, a moduli theory of properly immersed triply periodic minimal surfaces in $\mathbb{R}^3$ was established by the first author ([1], [2]). We can classify a key space of the moduli space into many connected components by the Morse index and nullity. Boundaries of the connected components may consist of properly immersed triply periodic minimal surfaces with non-trivial Jacobi fields, properly immersed doubly periodic minimal surfaces, properly immersed singly periodic minimal surfaces, and properly immersed minimal surfaces in $\mathbb{R}^3$. In the present paper, we consider two important periodic minimal surfaces which are contained in the boundaries, namely, Rodríguez' standard example (the doubly periodic case) and Karcher's saddle tower (the singly periodic case). We refer to related topics to doubly periodic minimal surfaces and singly periodic minimal surfaces in the next paragraph.

Lazard-Holly and Meeks [9] proved that if the quotient surface of a properly embedded doubly periodic minimal surface in $\mathbb{R}^3$ has genus 0, then the surface must be a doubly periodic Scherk minimal surface up to translations, rotations, and homotheties. In the higher genus case, Karcher [7] constructed one-parameter family of doubly periodic minimal surfaces, called *troidal half-plane layers*, with genus 1 and four Scherk-type parallel ends in its smallest fundamental domain. He also exposed two distinct one-parameter deformations of each troidal half-plane layer and so obtained other doubly periodic minimal tori with parallel ends. In 2007, Rodríguez [12] generalized these Karcher's examples which is called *a standard example*. Furthermore, Pérez, Rodríguez, and Traizet [11] showed that if the quotient surface of a properly embedded doubly periodic minimal surface in $\mathbb{R}^3$ has genus 1 and parallel ends, then the surface must be a standard example. For Karcher's saddle tower, the similar characterization is known. In fact, Pérez and Traizet [10] proved that the quotient surface of a properly embedded singly periodic minimal surface in $\mathbb{R}^3$ has genus 0 and six Scherk-type ends, then the surface must be Karcher's saddle tower. Note that Karcher's saddle tower has $2k$ Scherk-type ends for $k \geq 3$, and we now focus on the case $k = 3$. We shall prove that these two types of periodic minimal surfaces can be obtained as

limits of suitable families of properly immersed triply periodic minimal surfaces in $\mathbb{R}^3$. Next we refer to such families, called *Meeks' family*, *H family*, and *hCLP family*.

A properly immersed triply periodic minimal surface in $\mathbb{R}^3$ can be considered as a compact minimal surface in a flat three torus. In 1990, Meeks [5] constructed two real five dimensional families of embedded hyperelliptic minimal surfaces of genus 3 in three dimensional flat tori. These are the surfaces which can be represented as two-sheeted covers of S^2 branched over four pairs of antipodal points. H family was discovered by Schwarz [13] in 1800s. It is one-parameter family of hyperelliptic minimal surfaces of genus 3 in three dimensional flat tori which are not contained in Meeks' family. On the other hand, chemists Fogden and Hyde [3] considered many important families of compact minimal surfaces in three dimensional flat tori. hCLP family is one of the families which is not contained in Meeks' family as well. Now we state our main results as follows.

Theorem 1.1. *Any Rodríguez' standard example can be obtained as a limit of Meeks' examples.*

Theorem 1.2. *Karcher's saddle tower of six ends can be obtained as a limit of Schwarz' H surfaces. Furthermore, Karcher's saddle tower of six ends or its conjugate surface can be obtained as limits of hCLP family.*

Fogden and Hyde determined the representation formula of hCLP family. However, a mathematical proof for well-definedness might not be given. Thus we consider this problem and our result is

Theorem 1.3. *hCLP family is well-defined as one-parameter family of compact minimal surfaces of genus* 3 *in three dimensional flat tori. Furthermore, every minimal surface which is contained in hCLP family has well-defined conjugate surface.*

2 Preliminary

Let $f : M \to \mathbb{R}^3/\Lambda$ be a minimal immersion of a 2-manifold M into the flat three manifold $\mathbb{R}^3/\Lambda$ and we usually call $f(M)$ *a minimal surface* in $\mathbb{R}^3/\Lambda$. We will always take the minimal surface to be oriented. The isothermal coordinates make M into a Riemann surface and f is called *a conformal minimal immersion*. The following representation formula is one of basic tools for conformal minimal immersions:

Theorem 2.1 (Weierstrass representation)**.** *Let $f : M \to \mathbb{R}^3/\Lambda$ be a conformal minimal immersion. Then, up to translations, f can be represented as follows*:

$$f(p) = \Re \int_{p_0}^{p} \begin{pmatrix} (1-g^2)\eta \\ i(1+g^2)\eta \\ 2g\eta \end{pmatrix} \mod \Lambda \tag{2.1}$$

where (g, η) is a pair of a meromorphic function g and a holomorphic differential η on the Riemann surface M so that

$$(1+|g|^2)^2 \eta\bar{\eta}$$

gives a Riemannian metric on M, and

$$\left\{ \Re \oint_{\ell} \begin{pmatrix} (1-g^2)\eta \\ i(1+g^2)\eta \\ 2g\eta \end{pmatrix} \;\middle|\; \ell \in H_1(M, \mathbb{Z}) \right\}$$

is contained in Λ. The meromorphic function g is called the Gauss map for the minimal surface.

Using the above formula, we list the minimal surfaces which we consider in this paper.

Example 2.1 (Meeks' family [5])**.** Let $a_1, \ldots, a_4$ be distinct complex numbers satisfying $a_1a_2a_3a_4 > 0$. Assume that any pair of a_j, a_k are not antipodal each other. Let M be the hyperelliptic Riemann surface of genus 3 defined by

$$w^2 = \prod_{j=1}^{4} (z - a_j) \left(z + \frac{1}{\overline{a_j}} \right).$$

Meeks' family consists of the following two minimal embeddings of M:

$$\Re \int_{p_0}^{p} \begin{pmatrix} 1-z^2 \\ i(1+z^2) \\ 2z \end{pmatrix} \frac{dz}{w}, \quad \Re \int_{p_0}^{p} i \begin{pmatrix} 1-z^2 \\ i(1+z^2) \\ 2z \end{pmatrix} \frac{dz}{w}.$$

Example 2.2 (Rodríguez' standard example [12])**.** Let M_θ be the Riemann surface defined by

$$w^2 = (z^2 + \lambda^2) \left(z^2 + \frac{1}{\lambda^2} \right) \tag{2.2}$$

where $\theta \in (0, \frac{\pi}{2})$ and $\lambda = \lambda(\theta) = \cot\frac{\theta}{2}$. Set

$$\sigma = \cos\frac{\alpha+\beta}{2} + i\cos\frac{\alpha-\beta}{2}, \quad \delta = \sin\frac{\alpha-\beta}{2} + i\sin\frac{\alpha+\beta}{2},$$

where $\alpha, \beta \in [0, \pi/2]$ are constants with $(\alpha, \beta) \neq (0, \theta)$. Let g be a meromorphic function on M_θ defined by

$$g(z, w) = \frac{\sigma z + \delta}{i(\overline{\sigma} - \overline{\delta} z)}.$$

The surface we will consider is

$$M = M_\theta \setminus g^{-1}(\{0, \infty\}).$$

Rodríguez' standard example is three-parameter family consists of the following conformal minimal embeddings of M:

$$\frac{\pi \csc\theta}{\kappa(\sin^2\theta)} \Re \int_{p_0}^{p} \begin{pmatrix} 1 - g^2 \\ i(1+g^2) \\ 2g \end{pmatrix} \frac{dz}{gw}, \tag{2.3}$$

where $\kappa(m) = \displaystyle\int_0^{\frac{\pi}{2}} \frac{du}{\sqrt{1 - m\sin^2 u}}$. We remark that the space of Rodríguez' standard example is self-conjugate, that is, the conjugate surface of any Rodríguez' standard example is also one of a Rodríguez' standard example.

Example 2.3 (H family [8])**.** For $a \in (0, 1)$, let M be the hyperelliptic Riemann surface of genus 3 defined by

$$w^2 = z(z^3 - a^3)\left(z^3 - \frac{1}{a^3}\right).$$

H family is one-parameter family consists of the following conformal minimal embeddings of M:

$$\Re \int_{p_0}^{p} i \begin{pmatrix} 1 - z^2 \\ i(1+z^2) \\ 2z \end{pmatrix} \frac{dz}{w}.$$

Example 2.4 (hCLP family [3])**.** For $\theta \in (0, \frac{\pi}{3})$, let M be the hyperelliptic Riemann surface of genus 3 defined by

$$w^2 = z(z^6 - 2\cos(3\theta)z^3 + 1). \tag{2.4}$$

hCLP family is one-parameter family consists of the following conformal minimal immersions of M:

$$\Re \int_{p_0}^{p} \begin{pmatrix} 1-z^2 \\ i(1+z^2) \\ 2z \end{pmatrix} \frac{dz}{w}.$$

Example 2.5 (Karcher's saddle tower [7])**.** Let M be the Riemann surface

$$(\mathbb{C} \cup \{\infty\}) \setminus \{\pm e^{\frac{\pi}{6}i}, \pm e^{-\frac{\pi}{6}i}, \pm i\}.$$

Karcher's saddle tower with six ends is the following conformal minimal embedding of M:

$$\Re \int_{p_0}^{p} \begin{pmatrix} 1-z^4 \\ i(1+z^4) \\ 2z^2 \end{pmatrix} \frac{dz}{1+z^6}.$$

Example 2.6 (Schwarz' CLP surface [8])**.** Let M be the hyperelliptic Riemann surface of genus 3 defined by

$$w^2 = z^8 + 1.$$

Schwarz' CLP surface is the following conformal minimal embedding of M:

$$\Re \int_{p_0}^{p} \begin{pmatrix} 1-z^2 \\ i(1+z^2) \\ 2z \end{pmatrix} \frac{dz}{w}.$$

We remark that the conjugate surface of Schwarz' CLP surface is again Schwarz' CLP surface.

Example 2.7 (Riemann's minimal examples [4])**.** Let M_λ be the Riemann surface defined by

$$w^2 = z(z-\lambda)\left(z + \frac{1}{\lambda}\right).$$

The surface we will consider is

$$M = M_\lambda \setminus \{(0,\, 0),\, (\infty,\, \infty)\}.$$

The Weierstrass representation for the Riemann's minimal examples is :

$$\Re \int_{p_0}^{p} \begin{pmatrix} 1-z^2 \\ i(1+z^2) \\ 2z \end{pmatrix} \frac{dz}{zw}.$$

We remark that the conjugate surface of Riemann's minimal example is again Riemann's minimal example.

3 Proofs of Main Theorems

3.1 Proof of Theorem 1.1

First we treat Meeks' family. Let M be the Riemann surface defined in Example 2.1.

We consider a structure of M as a branched two-sheeted cover of S^2. Recall that the Gauss map $(z,\, w) \mapsto z$ gives rise to the branched two-sheeted cover of S^2 (see the proof of Corollary 3.2 in [5]). The branch locus of the Gauss map consists of the following eight points on S^2:

$$a_1,\ a_2,\ a_3,\ a_4,\ -\frac{1}{\overline{a_1}},\ -\frac{1}{\overline{a_2}},\ -\frac{1}{\overline{a_3}},\ -\frac{1}{\overline{a_4}}.$$

We prepare two copies of $\mathbb{C} \cup \{\infty\} \cong S^2$ and take two closed curves passing through the eight points, respectively. So we can divide S^2 into two domains and label " $+$ " and " $-$ " (see Figure 3.1). Slit thick curves as in the upper

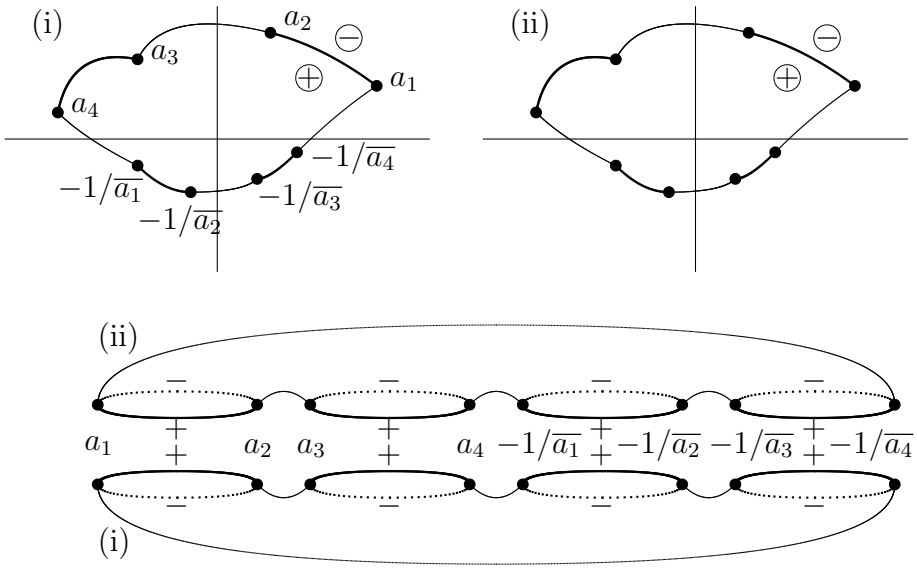

Figure 3.1: The hyperelliptic Riemann surface M of genus 3

pictures in Figure 3.1 and glue (i) and (ii) as in the lower pictures in Figure 3.1. The thin curves in the upper pictures in Figure 3.1 are corresponding to the thin curves in the lower pictures in Figure 3.1. By this procedure, we obtain the hyperelliptic Riemann surface M of genus 3.

We now consider the case $a_2 \to a_1$. Let α be a closed curve enclosing a_1 and a_2, β a closed curve enclosing $-1/\overline{a_1}$ and $-1/\overline{a_2}$ in the z-plane. Lift α and β to closed curves in M, name them $\hat{\alpha}$, $\hat{\alpha}'$, $\hat{\beta}$, and $\hat{\beta}'$. Choosing suitable α and β, we can divide M among three disjoint sets in M with the following properties: The first set contains $(a_1, 0)$ and $(a_2, 0)$ whose boundary consists of $\hat{\alpha}$ and $\hat{\alpha}'$, the second set contains $(-1/\overline{a_1}, 0)$ and $(-1/\overline{a_2}, 0)$ whose boundary consists of $\hat{\beta}$ and $\hat{\beta}'$, and the third set is the remaining set (see Figure 3.2). Name the third set $M_{\alpha\beta}$ with boundaries $\hat{\alpha}$, $\hat{\alpha}'$, $\hat{\beta}$, and $\hat{\beta}'$.

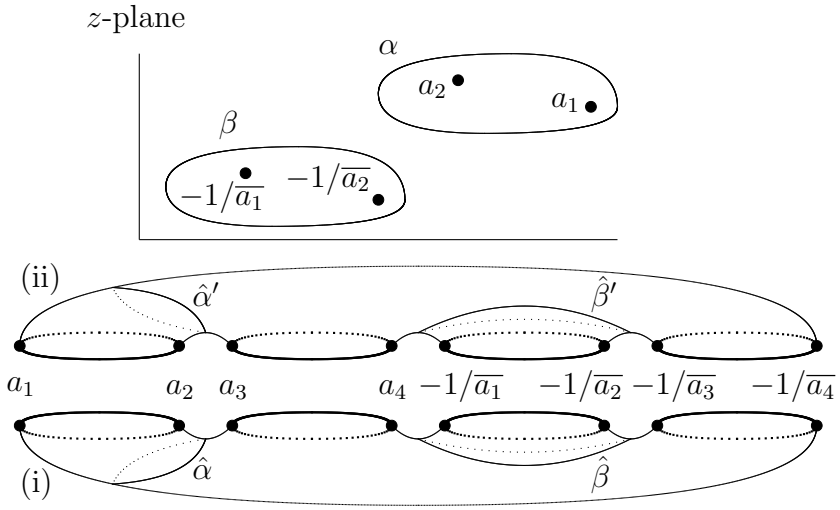

Figure 3.2: The hyperelliptic Riemann surface M of genus 3

The Weierstrass integral (2.1) along any closed curve in $M_{\alpha\beta}$ is contained in the lattice of the target torus. So the Weierstrass integral depends only on the endpoint of a path in $M_{\alpha\beta}$. We now assume $p_0 \in M_{\alpha\beta}$. Taking t as a local complex coordinate on $M_{\alpha\beta}$, we can write

$$\frac{1-z^2}{w}dz = \varphi_1(t)dt,\ \frac{i(1+z^2)}{w}dz = \varphi_2(t)dt,\ \frac{2z}{w}dz = \varphi_3(t)dt$$

for some holomorphic functions $\varphi_1(t)$, $\varphi_2(t)$, $\varphi_3(t)$. Then, the three functions $\varphi_1(t)$, $\varphi_2(t)$, $\varphi_3(t)$ converge uniformly on $M_{\alpha\beta}$ as $a_2 \to a_1$. Hence the limits can be moved inside the integrals. The similar arguments are given by Hoffman and Rossman's work [4].

As $a_2 \to a_1$, M converges to the following torus with nodes:

$$w^2 = (z-a_1)^2 \left(z + \frac{1}{\overline{a_1}}\right)^2 \prod_{j=3}^{4} (z-a_j)\left(z+\frac{1}{\overline{a_j}}\right).$$

We denote this torus with nodes by M'. Define the torus N by

$$W^2 = \prod_{j=3}^{4} (z-a_j)\left(z+\frac{1}{\overline{a_j}}\right). \tag{3.1}$$

Then there exists the following reparametrization of M':

$$\begin{array}{ccc} N & \longrightarrow & M' \\ (z,\, W) & \longmapsto & \left(z,\, (z-a_1)\left(z+\dfrac{1}{\overline{a_1}}\right) W\right) \end{array}$$

By using them, the limits, as $a_2 \to a_1$, of the representations of two minimal embeddings of M are

$$\Re \int_{p_0}^{p} (1-z^2,\, i(1+z^2),\, 2z)^t \frac{1}{(z-a_1)(z+\frac{1}{\overline{a_1}})W} dz, \tag{3.2}$$

$$\Im \int_{p_0}^{p} (1-z^2,\, i(1+z^2),\, 2z)^t \frac{1}{(z-a_1)(z+\frac{1}{\overline{a_1}})W} dz \tag{3.3}$$

on N, where $a_1^2 a_3 a_4 > 0$. We set $a_1 = re^{i\eta}$. To find sequences of them, we renormalize them by a homothetic transformation r:

$$\begin{aligned} & r \int_{p_0}^{p} (1-z^2,\, i(1+z^2),\, 2z)^t \frac{1}{(z-re^{i\eta})(z+\frac{e^{i\eta}}{r})W} dz \\ &= \int_{p_0}^{p} (1-z^2,\, i(1+z^2),\, 2z)^t \frac{1}{(\frac{z}{r}-e^{i\eta})(z+\frac{e^{i\eta}}{r})W} dz. \end{aligned}$$

It follows that, as $r \to \infty$, this converges to

$$-\int_{p_0}^{p} (1-z^2,\, i(1+z^2),\, 2z)^t \frac{1}{e^{i\eta} z W} dz \quad (e^{2i\eta} a_3 a_4 > 0)$$

Hence, up to homotheties, (3.2) and (3.3) converge to

$$-\Re \int_{p_0}^{p} (1-z^2,\, i(1+z^2),\, 2z)^t \frac{1}{e^{i\eta} z W} dz, \tag{3.4}$$

$$-\Im \int_{p_0}^{p} (1-z^2,\, i(1+z^2),\, 2z)^t \frac{1}{e^{i\eta} z W} dz, \tag{3.5}$$

where $e^{2i\eta}a_3a_4 > 0$. Note that the Gauss map at the ends go to 0 or ∞ when r goes to infinity.

Next, we consider the Rodríguez' standard example. Let M'' be the torus defined in Example 2.2. Substituting in the expression (2.2) for $z = \frac{-\delta+i\overline{\sigma}g}{\sigma+i\overline{\delta}g}$, we have

$$(\sigma+i\overline{\delta}g)^4w^2 = (\overline{\sigma}^2+\lambda^2\overline{\delta}^2)\left(\overline{\sigma}^2+\frac{\overline{\delta}^2}{\lambda^2}\right)\left(g-\frac{\delta+i\lambda\sigma}{i\overline{\sigma}+\lambda\overline{\delta}}\right) \times\left(g-\frac{\delta-i\lambda\sigma}{i\overline{\sigma}-\lambda\overline{\delta}}\right)\left(g-\frac{\lambda\delta+i\sigma}{i\lambda\overline{\sigma}+\overline{\delta}}\right)\left(g-\frac{\lambda\delta-i\sigma}{i\lambda\overline{\sigma}-\overline{\delta}}\right). \tag{3.6}$$

Also, we find $dz = \frac{i(|\sigma|^2+|\delta|^2)}{(\sigma+i\overline{\delta}g)^2}dg = \frac{2i}{(\sigma+i\overline{\delta}g)^2}dg$. Thus (2.3) can be written in the form

$$-\frac{2\pi\csc\theta}{\kappa(\sin^2\theta)}\Im\int_{p_0}^{p}(1-g^2,\, i(1+g^2),\, 2g)^t\frac{dg}{g(\sigma+i\overline{\delta}g)^2w}. \tag{3.7}$$

By setting

$$a_3 = \frac{\delta+i\lambda\sigma}{i\overline{\sigma}+\lambda\overline{\delta}}, \quad a_4 = \frac{\lambda\delta+i\sigma}{i\lambda\overline{\sigma}+\overline{\delta}}, \tag{3.8}$$

(3.6) takes the form

$$(\sigma+i\overline{\delta}g)^4w^2 = (\overline{\sigma}^2+\lambda^2\overline{\delta}^2)\left(\overline{\sigma}^2+\frac{\overline{\delta}^2}{\lambda^2}\right)\prod_{j=3}^{4}(g-a_j)\left(g+\frac{1}{\overline{a_j}}\right).$$

Now, let T be the torus defined by

$$V^2 = \prod_{j=3}^{4}(g-a_j)\left(g+\frac{1}{\overline{a_j}}\right). \tag{3.9}$$

Setting $\ell e^{iq} = \sqrt{(\overline{\sigma}^2+\lambda^2\overline{\delta}^2)(\overline{\sigma}^2+\frac{\overline{\delta}^2}{\lambda^2})}$ for a suitable branch of $\sqrt{*}$, we have the following biholomorphism:

$$\begin{array}{ccc} T & \longrightarrow & M'' \\ (g,\, V) & \longmapsto & \left(g,\, \dfrac{\ell e^{iq}V}{(\sigma+i\overline{\delta}g)^2}\right) \end{array}$$

So we can write (3.7) in the form

$$-\frac{2\pi\csc\theta}{\ell\kappa(\sin^2\theta)}\,\Im\int_{p_0}^{p}(1-g^2,\,i(1+g^2),\,2g)^t\frac{dg}{ge^{iq}V}. \tag{3.10}$$

Note that

$$e^{2iq}a_3a_4=\frac{1}{\lambda^2}|\lambda\delta+i\sigma|^2|\delta+i\lambda\sigma|^2>0.$$

Therefore, by (3.1), (3.5), (3.9), and (3.10), we can see that the standard example associated to λ, δ, σ can be obtained as a limit of Meeks' family (up to blowing up) with a_3, a_4 as in (3.8) when $a_2\to a_1$ and $|a_1|\to\infty$.

3.2 Proof of Theorem 1.2

The following arguments are quite similar to § 3.1. First we consider H family. The limit, as $a\to 1$, of M defined in Example 2.3 is the Riemann surface with nodes given by $w^2=z(z^3-1)^2$. Let M' be this Riemann surface with nodes, then there exists a reparametrization of M':

$$\begin{array}{ccc} S^2 & \longrightarrow & M' \\ u & \longmapsto & (-u^2,\,-iu(u^6+1)) \end{array}$$

Correspondingly, the limit of the representation is

$$2\begin{pmatrix}1&0&0\\0&1&0\\0&0&-1\end{pmatrix}\Re\int_{p_0}^{p}\begin{pmatrix}1-u^4\\i(1+u^4)\\2u^2\end{pmatrix}\frac{du}{u^6+1}$$

on $(\mathbb{C}\cup\{\infty\})\setminus\{\pm e^{\frac{\pi}{6}i},\,\pm e^{-\frac{\pi}{6}i},\,\pm i\}$. Hence we conclude that H family converges to Karcher's saddle tower of six ends.

Next we treat hCLP family. The limit, as $\theta\to 0$, of M defined in Example 2.4 is the Riemann surface with nodes given by $w^2=z(z^3-1)^2$ and the limit, as $\theta\to\frac{\pi}{3}$, of M is the Riemann surface with nodes given by $w^2=z(z^3+1)^2$. For the former case, we can apply the same arguments as above, and we find that the limit of hCLP family is the conjugate surface of Karcher's saddle tower. In the latter case, hCLP family converges to Karcher's saddle tower because it must be the conjugate surface up to a symmetry for the former case as seen in the next subsection.

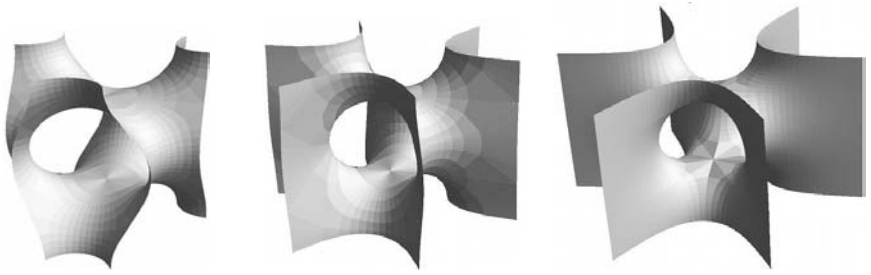

H family ($a = 0.5$) H family ($a = 0.9$) Karcher's tower

Figure 3.3: Behavior for the case $a \to 1$

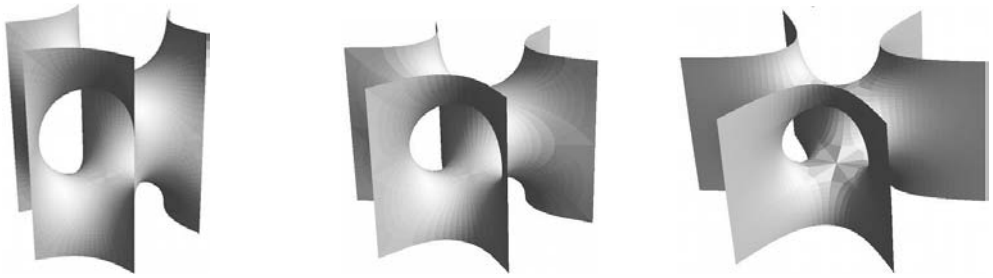

hCLP family ($\theta = \pi/6$) hCLP family ($\theta = 7\pi/24$) Karcher's tower

Figure 3.4: Behavior for the case $\theta \to \frac{\pi}{3}$

3.3 Proof of Theorem 1.3

In this subsection, we give a canonical homology basis of hCLP family and show that every minimal immersion defined in Example 2.4 is well-defined for an arbitrary $\theta \in (0,\, \frac{\pi}{3})$.

First we remark that we may assume $0 < \theta \leq \frac{\pi}{6}$. In fact, For $\theta \in [\frac{\pi}{6},\, \frac{\pi}{3})$, if we set $\varphi = \frac{\pi}{3} - \theta$, then we have $\varphi \in (0,\, \frac{\pi}{6}]$ and (2.4) takes the form

$$w^2 = z(z^6 + 2\cos(3\varphi)z^3 + 1). \tag{3.11}$$

Setting $(z,\, w) = (-\alpha,\, i\beta)$, we find

$$\begin{pmatrix} 1 - z^2 \\ i(1 + z^2) \\ 2z \end{pmatrix} \frac{dz}{w} = i \begin{pmatrix} 1 & 0 & 0 \\ 0 & 1 & 0 \\ 0 & 0 & -1 \end{pmatrix} \begin{pmatrix} 1 - \alpha^2 \\ i(1 + \alpha^2) \\ 2\alpha \end{pmatrix} \frac{d\alpha}{\beta}$$

and we write (3.11) in the form

$$\beta^2 = \alpha(\alpha^6 - 2\cos(3\varphi)\alpha^3 + 1).$$

Thus the minimal immersion for $\theta \in [\frac{\pi}{6},\, \frac{\pi}{3})$ can be reconsidered as the conjugate surface for $\theta \in (0,\, \frac{\pi}{6}]$ up to a symmetry. From now on, we assume $0 < \theta \leq \frac{\pi}{6}$.

To start with, we consider a structure of M as a branched two-sheeted cover of S^2. Recall that the Gauss map $(z,\, w) \mapsto z$ gives rise to the branched two-sheeted cover of S^2. The branch locus of the Gauss map consists of the following eight points on S^2:

$$0,\, \infty,\, e^{\pm i\theta},\, e^{\pm i(\theta \pm \frac{2}{3}\pi)}.$$

We prepare two copies of $\mathbb{C} \cup \{\infty\} \cong S^2$ and take two closed curves passing through the eight points, respectively. So we can divide S^2 into two domains and label " $+$ " and " $-$ " (see Figure 3.5).

Slit thick curves in Figure 3.5 and glue (i) and (ii) as in Figure 3.6. The thin curves in Figure 3.5 are corresponding to the thin curves in Figure 3.6. By this procedure, we obtain the hyperelliptic Riemann surface M of genus 3. Consider the biholomorphisms

$$j(z,\, w) = (z,\, -w), \quad \varphi(z,\, w) = (e^{\frac{2}{3}\pi i}z,\, e^{\frac{\pi}{3}i}w).$$

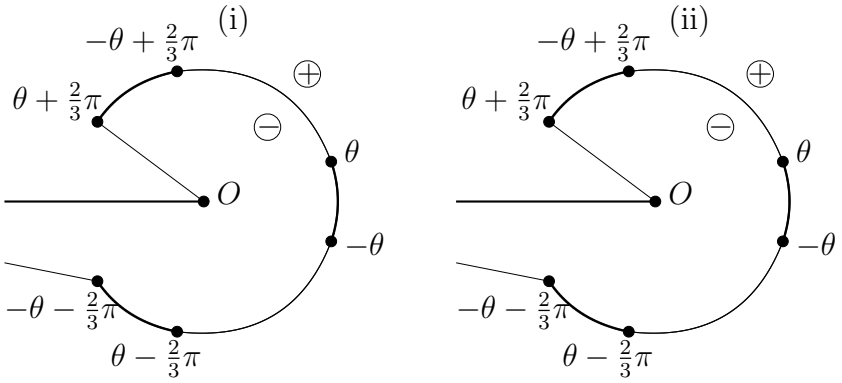

Figure 3.5: two copies of $\mathbb{C}\cup\{\infty\}$

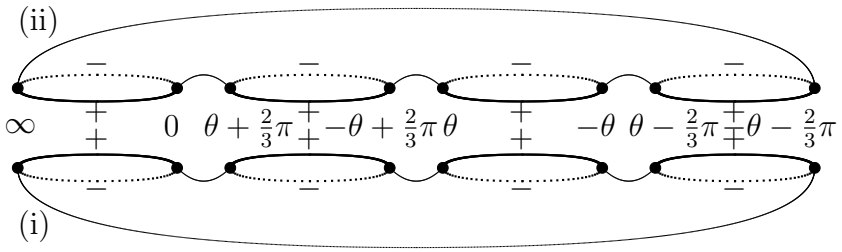

Figure 3.6: The hyperelliptic Riemann surface M of genus 3

j is the hyperelliptic involution and it can be considered as 180°-rotation around the horizontal axis between (i) and (ii) in Figure 3.6. Setting $G = (1-z^2,\, i(1+z^2),\, 2z)^t \frac{dz}{w}$, we have

$$j^*G = -G, \quad \varphi^*G = \begin{pmatrix} \frac{1}{2} & \frac{\sqrt{3}}{2} & 0 \\ -\frac{\sqrt{3}}{2} & \frac{1}{2} & 0 \\ 0 & 0 & -1 \end{pmatrix} G.$$

Let $\{C_j\}_{j=1}^4$ be the following key paths on M:

$$C_1 := \left\{ (z,\, w) = (e^{it},\, w(t)) \;\middle|\; t \in \left[\theta,\, -\theta + \frac{2}{3}\pi\right],\, w\left(\frac{\pi}{3}\right) \in -e^{\frac{\pi}{6}i}\mathbb{R}_{>0} \right\},$$
$$C_2 := \{(z,\, w) = (-t,\, i\sqrt{t(t^6 + 2\cos(3\theta)t^3 + 1)}\,) \mid t \in [0,\, \infty],\, \sqrt{*} > 0\},$$
$$C_3 := \{(z,\, w) = (e^{it},\, w(t)) \mid t \in [-\theta,\, \theta],\, w(0) > 0\},$$
$$C_4 := \{(z,\, w) = (t,\, \sqrt{t(t^6 - 2\cos(3\theta)t^3 + 1)}\,) \mid t \in [0,\, \infty],\, \sqrt{*} > 0\}.$$

Note that $t^6 \pm 2\cos(3\theta)t^3 + 1 = (t^3 \pm \cos(3\theta))^2 + \sin^2(3\theta) \geq 0$. Choose C_1 as in Figure 3.7, and we shall determine other paths.

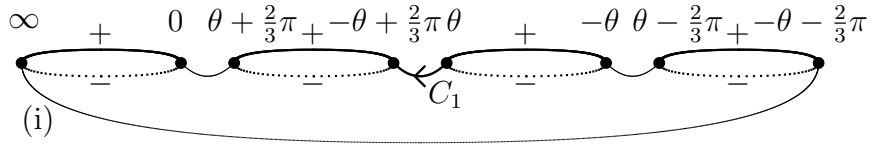

Figure 3.7: C_1 in (i)

Since $C_1 \cap \varphi^2(C_2) = \{(e^{\frac{\pi}{3}i},\, -e^{\frac{\pi}{6}i}\sqrt{2 + 2\cos(3\theta)}\,)\} \neq \emptyset$, $\varphi^2(C_2)$ lies on (i). There exist $m,\, n \in \{0,\, 1\}$ such that $j^m(\varphi(C_2)) - \varphi^2(C_2)$ is homotopic to $j^n(C_3 - j(C_3))$, written by $j^m(\varphi(C_2)) - \varphi^2(C_2) \sim j^n(C_3 - j(C_3))$ (see Figure 3.8).

To determine m and n, we now use their periods. Straightforward calcu-

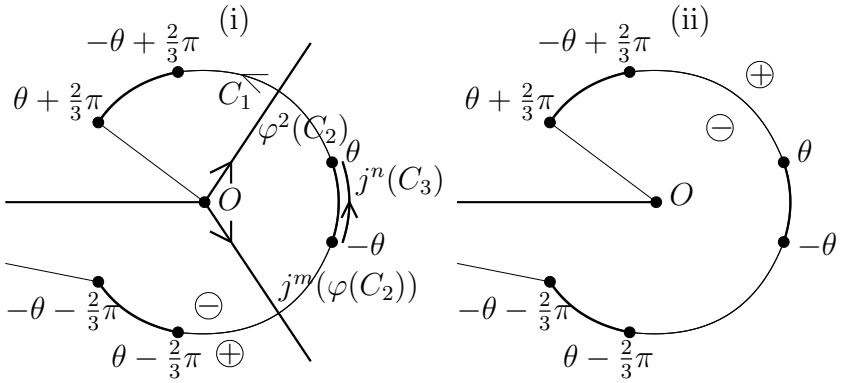

Figure 3.8: $j^m(\varphi(C_2)) - \varphi^2(C_2)$ and $j^n(C_3 - j(C_3))$

lations yield

$$\int_{C_2} \frac{1-z^2}{w} dz = i \int_0^\infty \frac{1-t^2}{\sqrt{t(t^6+2\cos(3\theta)t^3+1)}} dt = 0,$$
$$\int_{C_2} \frac{i(1+z^2)}{w} dz = -\int_0^\infty \frac{1+t^2}{\sqrt{t(t^6+2\cos(3\theta)t^3+1)}} dt,$$
$$\int_{C_2} \frac{2z}{w} dz = -2i \int_0^\infty \frac{t}{\sqrt{t(t^6+2\cos(3\theta)t^3+1)}} dt.$$

Next we compute periods along C_3. First we note that

$$\left(\frac{z^2}{w}\right)^2 = \frac{1}{z^3+\frac{1}{z^3}-2\cos(3\theta)} = \frac{1}{2\cos(3t)-2\cos(3\theta)}$$

on C_3. Since $0 < \theta \le \frac{\pi}{6}$, we have $(\frac{z^2}{w})^2 > 0$ on C_3. Moreover, $\frac{z^2}{w}(0) = \frac{1}{w(0)} > 0$ implies $\frac{z^2}{w} > 0$ on C_3. Set $x = \frac{1}{2}\left(z+\frac{1}{z}\right) = \cos t$. Then $z^3 + \frac{1}{z^3} = 8x^3 - 6x$ yields $\frac{z^2}{w} = \frac{1}{\sqrt{8x^3-6x-2\cos(3\theta)}}$. Hence

$$\int_{C_3} \frac{1-z^2}{w} dz = -2\int_{C_3} \frac{z^2}{w} dx$$
$$= -2\int_{\cos\theta}^1 \frac{dx}{\sqrt{8x^3-6x-2\cos(3\theta)}} - 2\int_1^{\cos\theta} \frac{dx}{\sqrt{8x^3-6x-2\cos(3\theta)}} = 0.$$

Note that

$$\frac{i(1+z^2)}{w} dz = \frac{2z^2}{w} \frac{i(z+\frac{1}{z})}{z-\frac{1}{z}} dx$$

and

$$\frac{i(z+\frac{1}{z})}{z-\frac{1}{z}} = \frac{1}{\tan t} = \begin{cases} -\dfrac{x}{\sqrt{1-x^2}} & (t \in [-\theta,\, 0]) \\ \dfrac{x}{\sqrt{1-x^2}} & (t \in [0,\, \theta]) \end{cases}$$

Thus we find

$$\begin{aligned} \int_{C_3} \frac{i(1+z^2)}{w} dz &= \int_{\cos\theta}^{1} \frac{-2x dx}{\sqrt{(8x^3-6x-2\cos(3\theta))(1-x^2)}} \\ &\quad + \int_{1}^{\cos\theta} \frac{2x dx}{\sqrt{(8x^3-6x-2\cos(3\theta))(1-x^2)}} \\ &= -4\int_{\cos\theta}^{1} \frac{x}{\sqrt{(8x^3-6x-2\cos(3\theta))(1-x^2)}} dx. \end{aligned}$$

Similarly,

$$\frac{2z}{w} dz = \frac{4z^2}{w} \frac{1}{z-\frac{1}{z}} dx$$

and

$$\frac{1}{z-\frac{1}{z}} = \frac{-i}{2\sin t} = \begin{cases} \dfrac{i}{2\sqrt{1-x^2}} & (t \in [-\theta,\, 0]) \\ -\dfrac{i}{2\sqrt{1-x^2}} & (t \in [0,\, \theta]) \end{cases}$$

imply

$$\begin{aligned} \int_{C_3} \frac{2z}{w} dz &= \int_{\cos\theta}^{1} \frac{2i dx}{\sqrt{(8x^3-6x-2\cos(3\theta))(1-x^2)}} \\ &\quad - \int_{1}^{\cos\theta} \frac{2i dx}{\sqrt{(8x^3-6x-2\cos(3\theta))(1-x^2)}} \\ &= 4i\int_{\cos\theta}^{1} \frac{dx}{\sqrt{(8x^3-6x-2\cos(3\theta))(1-x^2)}}. \end{aligned}$$

The equation $\int_{j^m(\varphi(C_2))-\varphi^2(C_2)} \frac{2z}{w} dz = \int_{j^n(C_3-j(C_3))} \frac{2z}{w} dz$ yields $m = n = 0$. So we have $\varphi(C_2) - \varphi^2(C_2) \sim C_3 - j(C_3)$. Also, we find

$$\int_0^\infty \frac{t}{\sqrt{t(t^6+2\cos(3\theta)t^3+1)}} dt = 2\int_{\cos\theta}^{1} \frac{dx}{\sqrt{(8x^3-6x-2\cos(3\theta))(1-x^2)}}. \tag{3.12}$$

Next the equation $\int_{\varphi(C_2)-\varphi^2(C_2)} \frac{i(1+z^2)}{w}dz = \int_{C_3-j(C_3)} \frac{i(1+z^2)}{w}dz$ implies

$$\int_0^\infty \frac{1+t^2}{\sqrt{t(t^6+2\cos(3\theta)t^3+1)}}dt = 8\int_{\cos\theta}^1 \frac{x}{\sqrt{(8x^3-6x-2\cos(3\theta))(1-x^2)}}dx. \tag{3.13}$$

Furthermore, we obtain the two figures as in Figure 3.9 in the process.

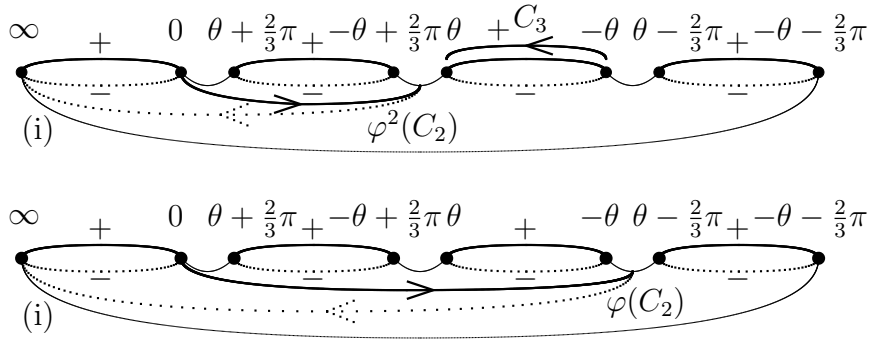

Figure 3.9: $\varphi(C_2)$, $\varphi^2(C_2)$, and C_3

Since $j(C_3) \cap j(C_4) = \{(1, -\sqrt{2-2\cos(3\theta)})\} \neq \emptyset$, $j(C_4)$ lies on "$-$" domain of (i). Thus we find two figures as in Figure 3.10.

Next, we see that there exists $m \in \{0, 1\}$ such that $j^m(\varphi(C_4)) - j(C_4) \sim C_1 - j(C_1)$. We shall determine m by periods. To start with, we find

$$\int_{C_4} \frac{1-z^2}{w}dz = \int_0^\infty \frac{1-t^2}{\sqrt{t(t^6-2\cos(3\theta)t^3+1)}}dt = 0,$$
$$\int_{C_4} \frac{i(1+z^2)}{w}dz = i\int_0^\infty \frac{1+t^2}{\sqrt{t(t^6-2\cos(3\theta)t^3+1)}}dt,$$
$$\int_{C_4} \frac{2z}{w}dz = 2\int_0^\infty \frac{t}{\sqrt{t(t^6-2\cos(3\theta)t^3+1)}}dt.$$

Note that

$$\left(\frac{z^2}{w}\right)^2 = \frac{1}{z^3+\frac{1}{z^3}-2\cos(3\theta)} = \frac{1}{2\cos(3t)-2\cos(3\theta)}$$

on C_1. Since $0 < \theta \leq \frac{\pi}{6}$, we have $(\frac{z^2}{w})^2 < 0$ on C_1. Also, since $\frac{z^2}{w}(\frac{\pi}{3}) = \frac{e^{\frac{2}{3}\pi i}}{w(\frac{\pi}{3})} \in -i\mathbb{R}_{>0}$, we find $\frac{z^2}{w} \in -i\mathbb{R}_{>0}$ on C_1. Set $x = \frac{1}{2}(z+\frac{1}{z}) = \cos t$. Then we have

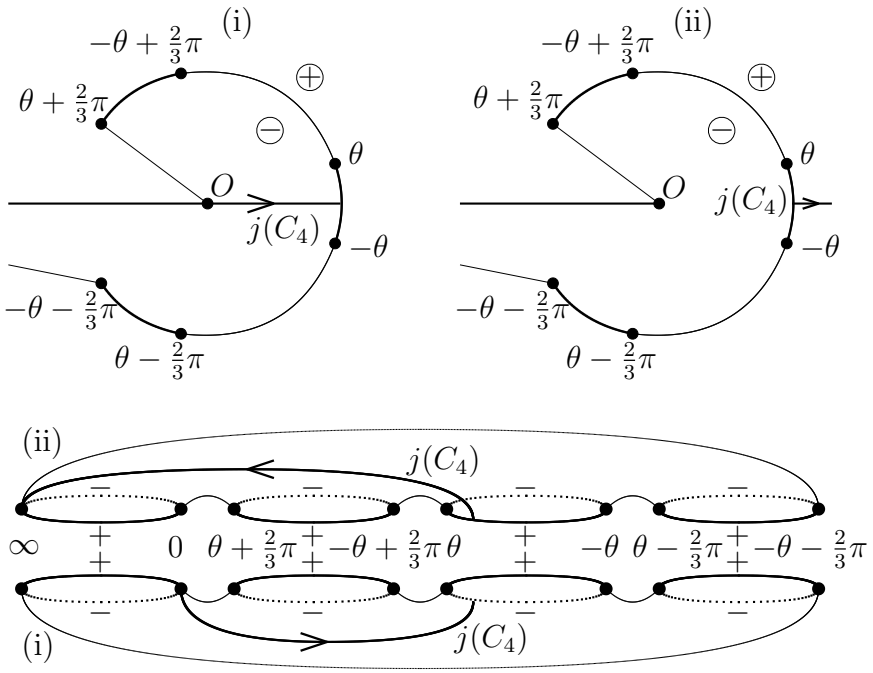

Figure 3.10: $j(C_4)$

$z^3+\frac{1}{z^3}=8x^3-6x$, and hence $\frac{z^2}{w}=-\frac{i}{\sqrt{2\cos(3\theta)+6x-8x^3}}$. It follows that

$$\int_{C_1}\frac{1-z^2}{w}dz=-2\int_{C_1}\frac{z^2}{w}dx=-2i\int_{\cos(-\theta+\frac{2}{3}\pi)}^{\cos\theta}\frac{dx}{\sqrt{2\cos(3\theta)+6x-8x^3}}.$$

Note that

$$\frac{i(1+z^2)}{w}dz=\frac{2z^2}{w}\frac{i(z+\frac{1}{z})}{z-\frac{1}{z}}dx$$

and

$$\frac{i(z+\frac{1}{z})}{z-\frac{1}{z}}=\frac{1}{\tan t}=\frac{x}{\sqrt{1-x^2}}.$$

So we find

$$\int_{C_1}\frac{i(1+z^2)}{w}dz=2i\int_{\cos(-\theta+\frac{2}{3}\pi)}^{\cos\theta}\frac{x}{\sqrt{(2\cos(3\theta)+6x-8x^3)(1-x^2)}}dx.$$

Similarly,

$$\frac{2z}{w}dz=\frac{4z^2}{w}\frac{1}{z-\frac{1}{z}}dx$$

and

$$\frac{1}{z-\frac{1}{z}} = \frac{-i}{2\sin t} = -\frac{i}{2\sqrt{1-x^2}}$$

imply

$$\int_{C_1} \frac{2z}{w} dz = 2\int_{\cos(-\theta+\frac{2}{3}\pi)}^{\cos\theta} \frac{dx}{\sqrt{(2\cos(3\theta)+6x-8x^3)(1-x^2)}}.$$

The equation $\int_{j^m(\varphi(C_4))-j(C_4)} \frac{2z}{w} dz = \int_{C_1-j(C_1)} \frac{2z}{w} dz$ yields $m = 1$, and thus $j(\varphi(C_4)) - j(C_4) \sim C_1 - j(C_1)$. In the process we also have

$$\int_0^\infty \frac{t}{\sqrt{t(t^6 - 2\cos(3\theta)t^3 + 1)}} dt = \int_{\cos(-\theta+\frac{2}{3}\pi)}^{\cos\theta} \frac{dx}{\sqrt{(2\cos(3\theta)+6x-8x^3)(1-x^2)}}. \tag{3.14}$$

The equation $\int_{j(\varphi(C_4))-j(C_4)} \frac{1-z^2}{w} dz = \int_{C_1-j(C_1)} \frac{1-z^2}{w} dz$ implies

$$\sqrt{3}\int_0^\infty \frac{1+t^2}{\sqrt{t(t^6 - 2\cos(3\theta)t^3 + 1)}} dt = 8\int_{\cos(-\theta+\frac{2}{3}\pi)}^{\cos\theta} \frac{dx}{\sqrt{2\cos(3\theta)+6x-8x^3}}. \tag{3.15}$$

Also, it follows from $\int_{j(\varphi(C_4))-j(C_4)} \frac{i(1+z^2)}{w} dz = \int_{C_1-j(C_1)} \frac{i(1+z^2)}{w} dz$ that

$$\int_0^\infty \frac{1+t^2}{\sqrt{t(t^6 - 2\cos(3\theta)t^3 + 1)}} dt = 8\int_{\cos(-\theta+\frac{2}{3}\pi)}^{\cos\theta} \frac{x}{\sqrt{(2\cos(3\theta)+6x-8x^3)(1-x^2)}} dx. \tag{3.16}$$

By these arguments, we find Figure 3.11.

Since $j(\varphi^2(C_1)) \cap \varphi(C_2) = (-e^{\frac{2}{3}\pi i}, ie^{\frac{\pi}{3}i}\sqrt{2+2\cos(3\theta)}) \neq \emptyset$, we have Figure 3.12.

There exist $m, n \in \{0, 1\}$ such that $\varphi^2(C_2) - j^m(C_2) \sim j^n(\varphi(C_3) - j(\varphi(C_3)))$. Since $\varphi(C_2) - \varphi^2(C_2) \sim C_3 - j(C_3)$, we find $\varphi^2(C_2) - j(C_2) \sim \varphi(C_3) - j(\varphi(C_3))$. Hence we have $m = 1$ and $n = 0$. So we obtain Figure 3.13.

Therefore, we can conclude that a canonical homology basis on M can be given by

$$A_1 = j(\varphi(C_4)) - C_2, \quad A_2 = -C_1 + j(C_1), \quad A_3 = \varphi^2(C_1) - j(\varphi^2(C_1)),$$
$$B_1 = -C_2 + j(C_2), \quad B_2 = \varphi^2(C_2) - C_2, \quad B_3 = \varphi(C_2) - C_2.$$

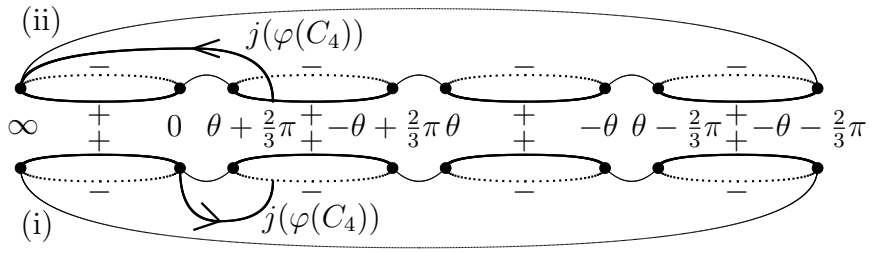

Figure 3.11: $j(\varphi(C_4))$

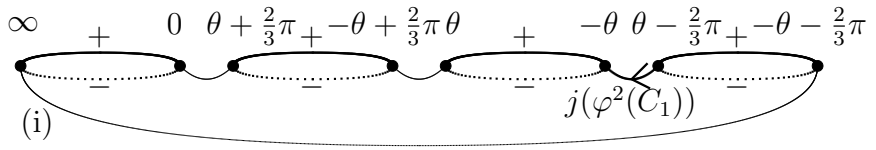

Figure 3.12: $j(\varphi^2(C_1))$

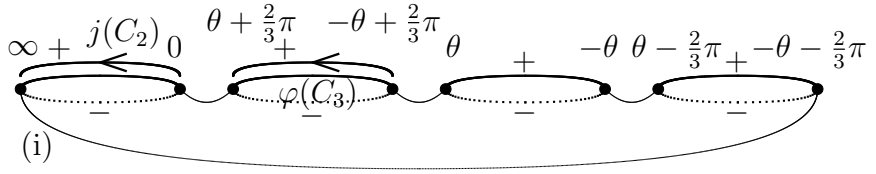

Figure 3.13: $j(C_2)$ and $\varphi(C_3)$

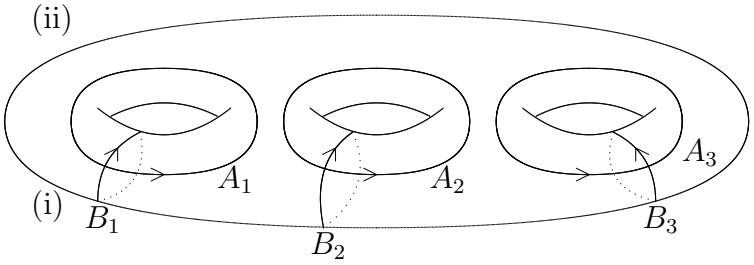

Figure 3.14: a canonical homology basis on M

By setting

$$A = \frac{1}{2}\int_0^\infty \frac{1+t^2}{\sqrt{t(t^6+2\cos(3\theta)t^3+1)}}dt,$$
$$B = \frac{1}{2}\int_0^\infty \frac{1+t^2}{\sqrt{t(t^6-2\cos(3\theta)t^3+1)}}dt,$$
$$C = 2\int_0^\infty \frac{t}{\sqrt{t(t^6-2\cos(3\theta)t^3+1)}}dt,$$
$$D = 2\int_0^\infty \frac{t}{\sqrt{t(t^6+2\cos(3\theta)t^3+1)}}dt,$$

and (3.12)–(3.16), the complex period matrix

$$\left(\int_{A_1} G, \int_{A_2} G, \int_{A_3} G, \int_{B_1} G, \int_{B_2} G, \int_{B_3} G\right)$$

is obtained by

$$\begin{pmatrix} -\sqrt{3}iB & \sqrt{3}iB & \sqrt{3}iB & 0 & -\sqrt{3}A & -\sqrt{3}A \\ 2A-iB & -iB & iB & 4A & 3A & A \\ C+iD & -2C & 2C & 2iD & 0 & 2iD \end{pmatrix}.$$

Taking real and imaginary parts of this, we find two lattices defined by

$$\Lambda = \begin{pmatrix} 2\sqrt{3}A & \sqrt{3}A & 0 \\ 0 & A & 0 \\ 0 & 0 & C \end{pmatrix}, \quad \Lambda' = \begin{pmatrix} 2\sqrt{3}B & \sqrt{3}B & 0 \\ 0 & B & 0 \\ 0 & 0 & D \end{pmatrix}.$$

As a result, we obtain a conformal minimal immersion of M

$$\begin{aligned} f \ &: M \longrightarrow \mathbb{R}^3/\Lambda \\ &p \longmapsto \Re \int_{p_0}^{p} (1-z^2,\, i(1+z^2),\, 2z)^t \frac{dz}{w} \end{aligned}$$

and this immersion gives hCLP family. Moreover, the conjugate surface

$$\begin{aligned} f \ &: M \longrightarrow \mathbb{R}^3/\Lambda' \\ &p \longmapsto \Re \int_{p_0}^{p} i(1-z^2,\, i(1+z^2),\, 2z)^t \frac{dz}{w} \end{aligned}$$

is also well-defined.

4 Examples in Theorem 1.1

In this section, we introduce three-parameter family of minimal surfaces which belongs to Meeks' family. This family contains CLP surface and we deform from CLP surface to Rodríguez' standard example. Then we further deform from Rodríguez' standard example to a singly periodic Riemann's minimal surface.

For z_1, z_2, $z_3 \in \mathbb{R}$, let M be the hyperelliptic Riemann surface of genus 3 defined by

$$w^2 = z\prod_{j=1}^{3}(z - z_j)\left(z + \frac{1}{z_j}\right). \tag{4.1}$$

We may assume that $0 < z_1 < z_3 < z_2 < \infty$. We now consider the following conformal minimal embeddings of M which belong to Meeks' family for the case $a_4 = 0$ or $a_4 = \infty$ in Example 2.1:

$$f(p) = \Re\int_{p_0}^{p}\begin{pmatrix}1 - z^2\\ i(1 + z^2)\\ 2z\end{pmatrix}\frac{dz}{w}, \quad f^*(p) = \Im\int_{p_0}^{p}\begin{pmatrix}1 - z^2\\ i(1 + z^2)\\ 2z\end{pmatrix}\frac{dz}{w}. \tag{4.2}$$

By letting z_3 tends to z_1, (4.1) is written as

$$w^2 = z(z - z_1)^2(z - z_2)\left(z + \frac{1}{z_1}\right)^2\left(z + \frac{1}{z_2}\right).$$

Setting $w = (z - z_1)\left(z + \frac{1}{z_1}\right)v$, we find that M tends to the torus T defined by

$$v^2 = z(z - z_2)\left(z + \frac{1}{z_2}\right).$$

By this reparametrization, (4.2) takes the form

$$f_T(p) = \Re\int_{p_0}^{p}\begin{pmatrix}1 - z^2\\ i(1 + z^2)\\ 2z\end{pmatrix}\frac{dz}{(z - z_1)\left(z + \frac{1}{z_1}\right)v}, \tag{4.3}$$

$$f_T^*(p) = \Im\int_{p_0}^{p}\begin{pmatrix}1 - z^2\\ i(1 + z^2)\\ 2z\end{pmatrix}\frac{dz}{(z - z_1)\left(z + \frac{1}{z_1}\right)v}, \tag{4.4}$$

on $T \setminus \{(z_1, *), (-1/z_1, *)\}$.

We now show that both of the above surfaces belong to Rodríguez standard example. Since $0 < z_1 < z_2 < \infty$, there exists $\varphi, \theta \in (0, \pi/2)$ so that

$$z_1 = \tan\varphi, \qquad z_2 = \tan\theta.$$

We set

$$\lambda = \cot\frac{\theta}{2}.$$

Let T_θ be a torus defined by

$$y^2 = (x^2 + \lambda^2)(x^2 + 1/\lambda^2).$$

Then we can identify T and T_θ with the biholomorphism

$$T_\theta \ni (x, y) \mapsto (z, v) = (z(x), v(x, y)) = \left(\frac{-\lambda x + i}{x + i\lambda}, -i\frac{(1+\lambda^2)\sqrt{z_2}}{2(x+i\lambda)^2}y\right) \in T.$$

It is easy to verify that $\dfrac{dz}{v} = \dfrac{2}{\sqrt{z_2}}\dfrac{dy}{x}$, thus (4.3) and (4.4) take the form

$$f_T(p) = \frac{2}{\sqrt{z_2}}\Re\int_{p_0}^{p}\begin{pmatrix}1-z^2\\ i(1+z^2)\\ 2z\end{pmatrix}\frac{dx}{(z-z_1)\left(z+\dfrac{1}{z_1}\right)y}, \tag{4.5}$$

$$f_T^*(p) = \frac{2}{\sqrt{z_2}}\Im\int_{p_0}^{p}\begin{pmatrix}1-z^2\\ i(1+z^2)\\ 2z\end{pmatrix}\frac{dx}{(z-z_1)\left(z+\dfrac{1}{z_1}\right)y}, \tag{4.6}$$

on $T_\theta \setminus z^{-1}(\{z_1, -1/z_1\})$. Now we rotate the surfaces by acting

$$A = \begin{pmatrix}\cos 2\varphi & 0 & \sin 2\varphi\\ 0 & 1 & 0\\ -\sin 2\varphi & 0 & \cos 2\varphi\end{pmatrix} \in SO(3).$$

Then the unit normal vectors are also rotate and

$$g(x) = (\pi \circ A \circ \pi^{-1})(z(x)) = \frac{\cos\varphi \cdot z(x) - \sin\varphi}{\sin\varphi \cdot z(x) + \cos\varphi} = \frac{z(x) - z_1}{z_1 z(x) + 1} \tag{4.7}$$

becomes the new Gauss map for both Af_T and Af_T^*, where $\pi : S^2 \to \mathbb{C} \cup \{\infty\}$ is the stereographic projection from the north pole S^2. By straightforward calculations yield that

$$Af_T(p) = \frac{2z_1}{(1+z_1^2)\sqrt{z_2}} \Re \int_{p_0}^{p} \begin{pmatrix} 1-g^2 \\ i(1+g^2) \\ 2g \end{pmatrix} \frac{dx}{gy}, \tag{4.8}$$

$$Af_T^*(p) = \frac{2z_1}{(1+z_1^2)\sqrt{z_2}} \Im \int_{p_0}^{p} \begin{pmatrix} 1-g^2 \\ i(1+g^2) \\ 2g \end{pmatrix} \frac{dx}{gy}. \tag{4.9}$$

on $T_\theta \setminus g^{-1}(\{0,\infty\})$. On the other hand, up to homothety, Rodríguez' standard example with $\alpha = 0$ is given by

$$f_R(p) = \Re \int_{p_0}^{p} \begin{pmatrix} 1-g_R^2 \\ i(1+g_R^2) \\ 2g_R \end{pmatrix} \frac{dx}{g_R y}$$

on $T_\theta \setminus g_R^{-1}(\{0,\infty\})$, where

$$g_R = \frac{-ix + \tan(\beta/2)}{\tan(\beta/2) \cdot x - i}.$$

If we rotate the surface by acting

$$B = \begin{pmatrix} 0 & -1 & 0 \\ 1 & 0 & 0 \\ 0 & 0 & 1 \end{pmatrix} \in SO(3),$$

then

$$g = ig_R = \frac{x + i\tan(\beta/2)}{\tan(\beta/2) \cdot x - i} \tag{4.10}$$

becomes the Gauss map for Bf_R, and we see that

$$Bf_R(p) = \Re \int_{p_0}^{p} \begin{pmatrix} 1-g^2 \\ i(1+g^2) \\ 2g \end{pmatrix} \frac{dx}{gy} \tag{4.11}$$

on $T_\theta \setminus g^{-1}(\{0,\infty\})$. Comparing (4.7) and (4.8) with (4.10) and (4.11), we see that (4.8) belongs to Rodríguez' standard example with

$$\theta = \tan^{-1} z_2, \qquad \alpha = 0, \qquad \beta = 2\tan^{-1} \frac{z_1\lambda - 1}{\lambda + z_1}.$$

Moreover, since the space of Rodríguez' standard example is self-conjugate as remarked in Example 2.2, (4.9) also belongs to Rodríguez' standard example.

Next we shall show that both of the families defined by (4.1) and (4.2) contain CLP surface. Here we only show the right hand side in (4.2) contains CLP surface. The other side can be shown by similar way. Set $\alpha = -\frac{z-i}{z+i}$ and $\alpha_j = \frac{-z_j+i}{z_j+i}$. Then we have $z = \frac{i(-\alpha+1)}{\alpha+1}$, and thus (4.1) takes the form

$$\{i(\alpha+1)^4 w\}^2 = (\alpha-1)(\alpha+1)\prod_{j=1}^{3}\left\{\frac{(z_j+i)^2}{z_j}(\alpha-\alpha_j)(\alpha+\alpha_j)\right\}. \quad (4.12)$$

By setting

$$i\beta\sqrt{\prod_{j=1}^{3}\frac{(z_j+i)^2}{z_j}} = (\alpha+1)^4 w$$

for suitable branches, (4.12) can be written as

$$\beta^2 = (\alpha-1)(\alpha+1)\prod_{j=1}^{3}\{(\alpha-\alpha_j)(\alpha+\alpha_j)\}. \quad (4.13)$$

Let $\tilde{M}$ be the Riemann surface defined by (4.13). On the other hand, (4.2) takes the form

$$f(p) = \begin{pmatrix} 0 & -1 & 0 \\ 0 & 0 & 1 \\ 1 & 0 & 0 \end{pmatrix} \Re \int_{p_0}^{p} \frac{4}{\sqrt{\prod_{j=1}^{3}\frac{(z_j+i)^2}{z_j}}} \begin{pmatrix} 1-\alpha^2 \\ i(1+\alpha^2) \\ 2\alpha \end{pmatrix} \frac{d\alpha}{\beta}.$$

Now we set $\tilde{f}(p) = \begin{pmatrix} 0 & -1 & 0 \\ 0 & 0 & 1 \\ 1 & 0 & 0 \end{pmatrix} \Re \int_{p_0}^{p} \begin{pmatrix} 1-\alpha^2 \\ i(1+\alpha^2) \\ 2\alpha \end{pmatrix} \frac{d\alpha}{\beta}$. For $\theta = \frac{\pi}{2} + \sum_{j=1}^{3}\frac{\arg\alpha_j}{2}$, we take an associate surface $\tilde{f}_\theta$ at angle θ of $\tilde{f}$:

$$\tilde{f}_\theta(p) = \Re \int_{p_0}^{p} e^{i\theta} \begin{pmatrix} 1-\alpha^2 \\ i(1+\alpha^2) \\ 2\alpha \end{pmatrix} \frac{d\alpha}{\beta}.$$

By the biholomorphism $\tilde{M} \to M$ defined by $(\alpha,\, \beta) \mapsto (z,\, w)$ as the above, we have the following diagram:

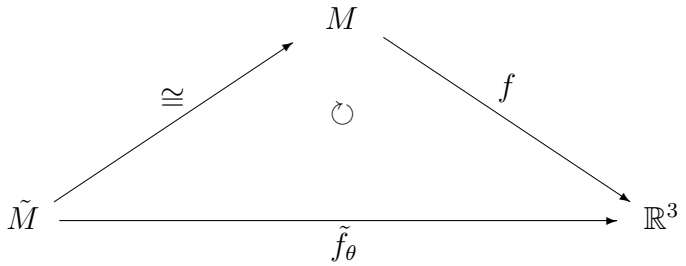

For the case $z_1 = \tan\frac{\pi}{8}$, $z_2 = \tan\frac{3}{8}\pi$, and $z_3 = \tan\frac{\pi}{4}$, $\tilde{M}$ is defined by $\beta^2 = \alpha^8 - 1$ and $\theta = \frac{5}{4}\pi$. By setting $\alpha = e^{\frac{\pi}{8}i}X$ and $\beta = iY$, $\tilde{M}$ is transformed to the Riemann surface given by $Y^2 = X^8 + 1$. Moreover, we find

$$e^{i\theta}\begin{pmatrix} 1-\alpha^2 \\ i(1+\alpha^2) \\ 2\alpha \end{pmatrix}\frac{d\alpha}{\beta} = -\begin{pmatrix} \cos\frac{\pi}{8} & -\sin\frac{\pi}{8} & 0 \\ \sin\frac{\pi}{8} & \cos\frac{\pi}{8} & 0 \\ 0 & 0 & 1 \end{pmatrix}\begin{pmatrix} 1-X^2 \\ i(1+X^2) \\ 2X \end{pmatrix}\frac{dX}{Y}$$

and therefore, we have CLP surface.

Figures 4.1 and 4.2 show the deformations from Schwarz' CLP surfaces (4.2) into Rodríguez standard examples.

Furthermore, we consider deformations of f_T and f_T^* given by (4.3) and (4.4) as $z_1 \to 0$. Straightforward calculation yields

$$\frac{1}{z_1}f_T(p) = \Re\int_{p_0}^{p}\begin{pmatrix} 1-z^2 \\ i(1+z^2) \\ 2z \end{pmatrix}\frac{dz}{(z-z_1)(z_1z+1)v}, \tag{4.14}$$

$$\frac{1}{z_1}f_T^*(p) = \Im\int_{p_0}^{p}\begin{pmatrix} 1-z^2 \\ i(1+z^2) \\ 2z \end{pmatrix}\frac{dz}{(z-z_1)(z_1z+1)v}. \tag{4.15}$$

For the case $z_1 = 0$, we have Riemann's minimal examples. Figures 4.3 and 4.4 show these deformations.

Remark 4.1. We set

$$\hat{f}_T(p) = \lim_{z_1\to 0}\frac{1}{z_1}f_T(p) = \Re\int_{p_0}^{p}\begin{pmatrix} 1-z^2 \\ i(1+z^2) \\ 2z \end{pmatrix}\frac{dz}{zv}, \tag{4.16}$$

$$\hat{f}_T^*(p) = \lim_{z_1\to 0}\frac{1}{z_1}f_T^*(p) = \Im\int_{p_0}^{p}\begin{pmatrix} 1-z^2 \\ i(1+z^2) \\ 2z \end{pmatrix}\frac{dz}{zv}. \tag{4.17}$$

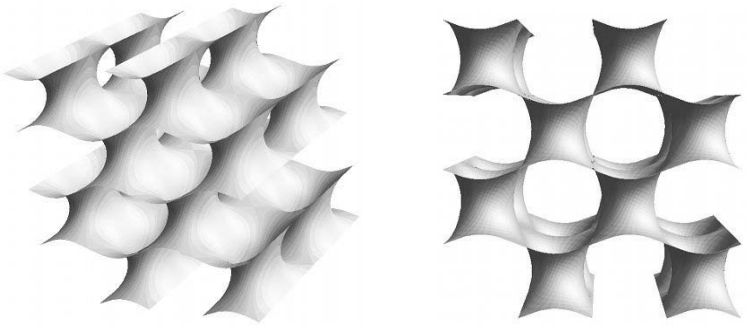

f for $(z_1,\, z_2,\, z_3) = (\sqrt{2}-1,\, \sqrt{2}+1,\, 1)$ (Schwarz' CLP)

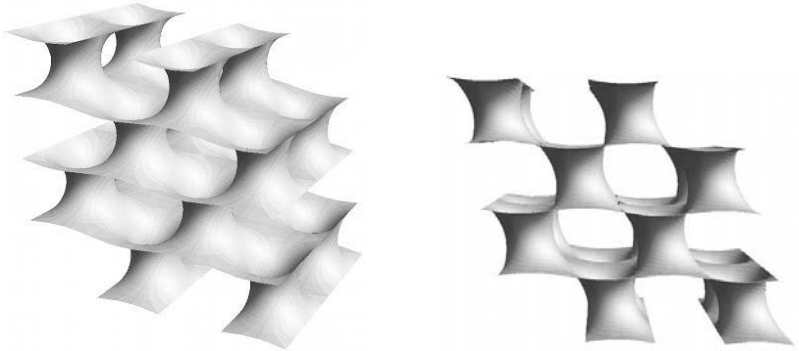

f for $(z_1,\, z_2,\, z_3) = (\sqrt{2}-1,\, \sqrt{2}+1,\, 0.6)$

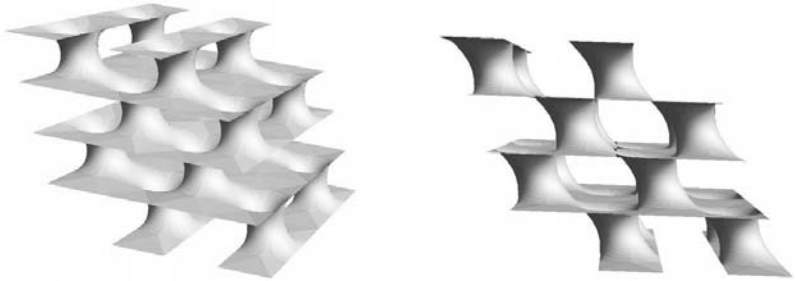

f for $(z_1,\, z_2,\, z_3) = (\sqrt{2}-1,\, \sqrt{2}+1,\, 0.42)$

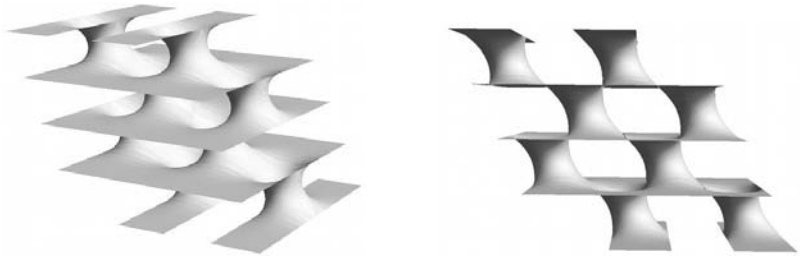

f_T for $(z_1,\, z_2) = (\sqrt{2}-1,\, \sqrt{2}+1)$ (Rodríguez)

Figure 4.1: Deformation from f to f_T as $z_3 \to z_1$.

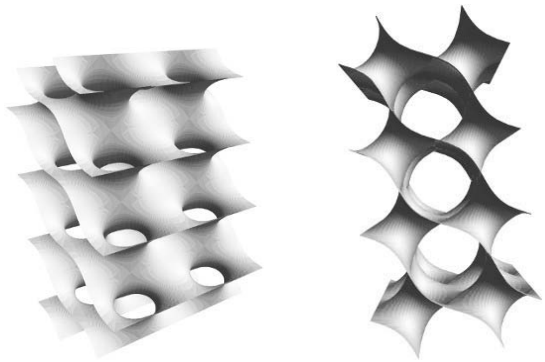

f^* for $(z_1,\, z_2,\, z_3) = (\sqrt{2}-1,\, \sqrt{2}+1,\, 1)$ (Schwarz' CLP)

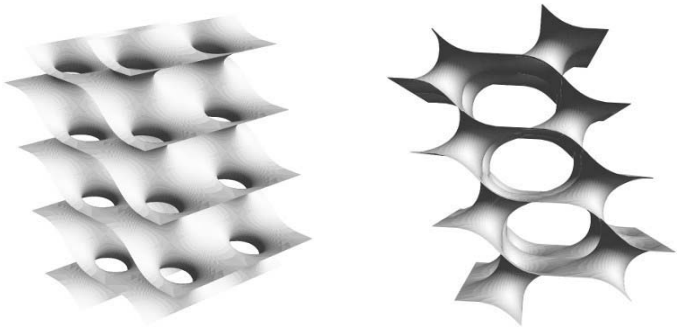

f^* for $(z_1,\, z_2,\, z_3) = (\sqrt{2}-1,\, \sqrt{2}+1,\, 0.6)$

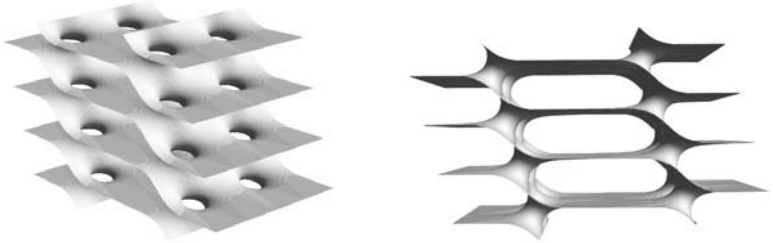

f^* for $(z_1,\, z_2,\, z_3) = (\sqrt{2}-1,\, \sqrt{2}+1,\, 0.42)$

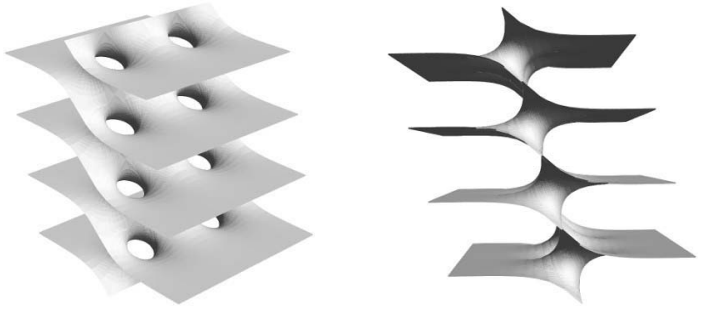

f_T^* for $(z_1,\, z_2) = (\sqrt{2}-1,\, \sqrt{2}+1)$ (Rodríguez)

Figure 4.2: Deformation from f^* to f_T^* as $z_3 \to z_1$.

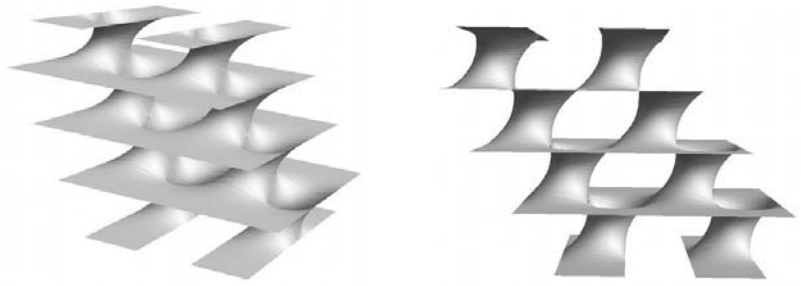

$\frac{1}{z_1} f_T$ for $(z_1, z_2) = (\sqrt{2} - 1, \sqrt{2} + 1)$

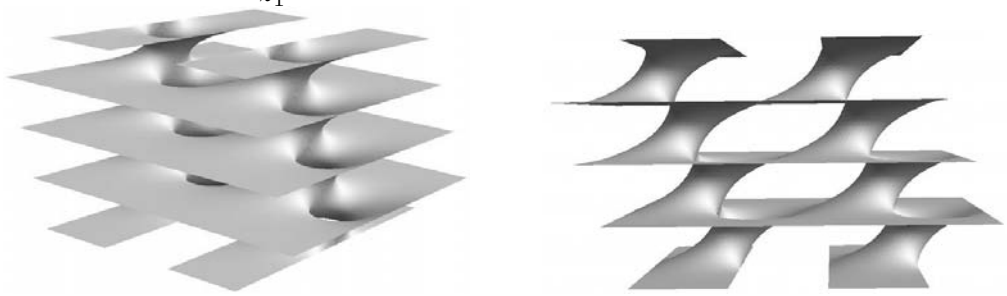

$\frac{1}{z_1} f_T$ for $(z_1, z_2) = (0.2, \sqrt{2} + 1)$

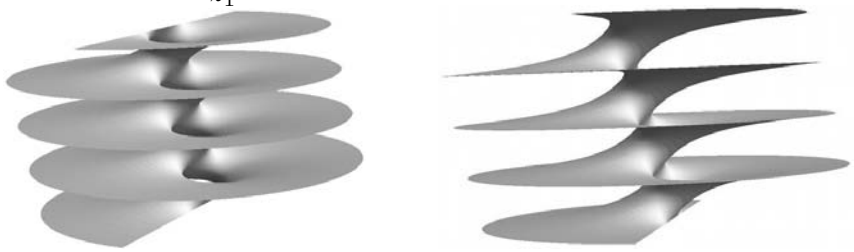

$\lim_{z_1 \to 0} \frac{1}{z_1} f_T$ for $z_2 = \sqrt{2} + 1$ (Riemann)

Figure 4.3: Deformation of $\frac{1}{z_1} f_T$ as $z_1 \to 0$.

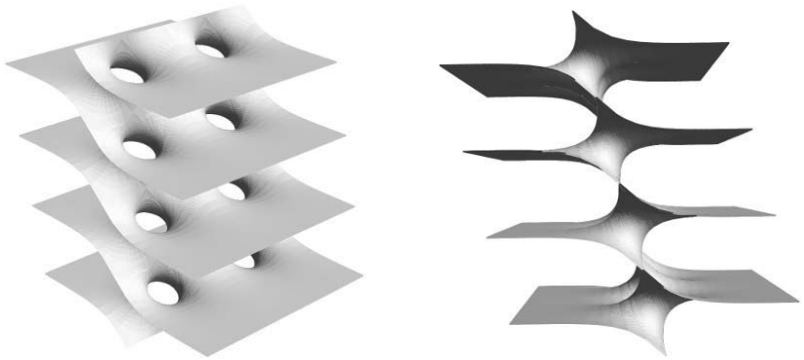

$\frac{1}{z_1} f_T^*$ for $(z_1,\, z_2) = (\sqrt{2}-1,\, \sqrt{2}+1)$

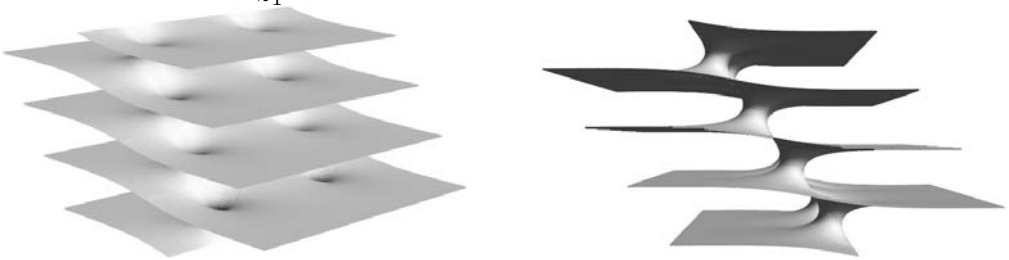

$\frac{1}{z_1} f_T^*$ for $(z_1,\, z_2) = (0.1,\, \sqrt{2}+1)$

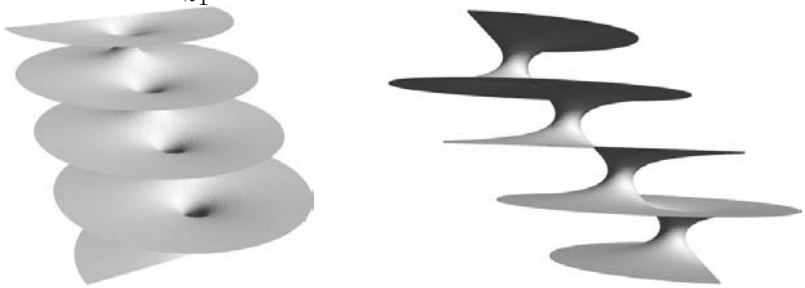

$\lim_{z_1 \to 0} \frac{1}{z_1} f_T^*$ for $z_2 = \sqrt{2}+1$ (Riemann)

Figure 4.4: Deformation of $\frac{1}{z_1} f_T^*$ as $z_1 \to 0$.

It is known that $\sqrt{z_2}\hat{f}_T$ (resp. $\sqrt{z_2}\hat{f}_T^*$) converges to the helicoid (resp. catenoid) as $z_2 \to \infty$. See [4]. Figure 4.5 shows these deformations.

Acknowledgement. The authors would like to thank the referee for valuable comments.

References

[1] N. Ejiri, *A differential-geometric Schottoky problem and minimal surfaces in tori*, Contemporary. Math. **308** (2002), 101–144.

[2] N. Ejiri and T. Shoda, *On a moduli theory of minimal surfaces*, Proceedings of the 3rd International Colloquium on Differential Geometry and Its Related Fields (2013), 155–172.

[3] A. Fogden and S. T. Hyde, *Parametrization of Triply Periodic Minimal Surfaces. ii. Regular Class Solutions*, Acta. Cryst. **A48** (1992), 575–591.

[4] D. Hoffman and W. Rossman, *Limit surfaces of Riemann examples*, The Journal of Geometric Analysis **7** (1997), no. 1, 161–171.

[5] W. H. Meeks III, *The Theory of Triply Periodic Minimal Surfaces*, Indiana U. Math. J. **39** (1990), no. 3, 877–936.

[6] W. H. Meeks III and H. Rosenberg, *The Geomety of Periodic Minimal Surfaces*, Comment. Math. Helvetici **68** (1993), 538–578.

[7] H. Karcher, *Embedded minimal surfaces derived from Scherk's examples*, Manuscripta Math. **62** (1988), 83–114.

[8] H. Karcher, *The triply periodic minimal surfaces of alan schoen and their constant mean curvature companions*, Manuscripta Math. **64** (1989), 291–357.

[9] H. Lazard-Holly and W. H. Meeks III, *Classification of doubly-periodic minimal surfaces of genus zero*, Invent. math. **143** (2001), 1–27.

[10] J. Pérez and M. Traizet, *The classification of singly periodic minimal surfaces with genus zero and Scherk-type ends*, Transactions of the American Mathematical Society **359** (2007), no. 3, 965–990.

$z_2 = \sqrt{2} + 1.$

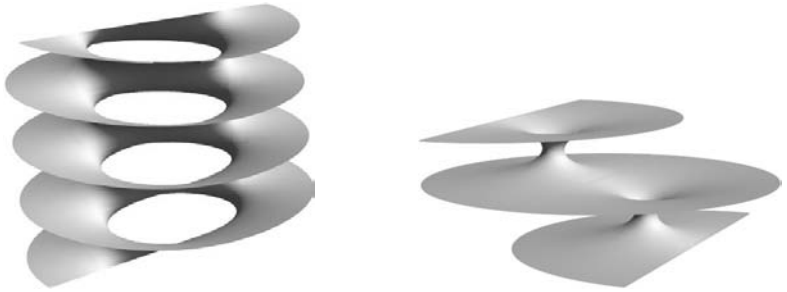

$z_2 = 5.$

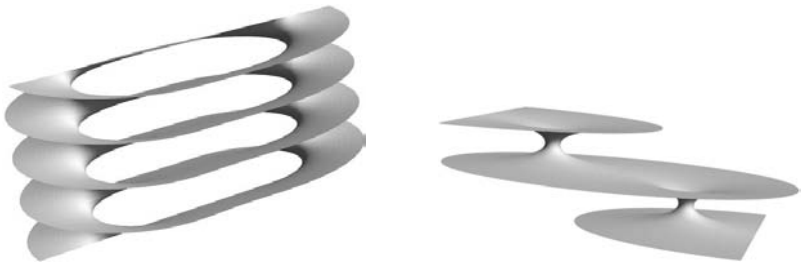

$z_2 = 10.$

Helicoid. Catenoid.

Figure 4.5: Left: Deformation of $\sqrt{z_1}\hat{f}_T$ as $z_2 \to \infty$. Right: Deformation of $\sqrt{z_1}\hat{f}_T^*$ as $z_2 \to \infty$.

[11] J. Pérez, M. M. Rodríguez, and M. Traizet, *The classification of doubly periodic minimal tori with parallel ends*, J. Differential Geometry **69** (2005), 523–577.

[12] M. M. Rodríguez, *The Space of Doubly Periodic Minimal Tori with Parallel Ends: Standard Examples*, Michigan Math. J. **55** (2007), 103–122.

[13] H. A. Schwarz, *Gesammelte Mathematische Abhandlungen, vol 1*, Berlin: Springer-Verlag (1890).

Norio Ejiri
Department of Mathematics, Meijo University
Tempaku, Nagoya 468-8502, Japan.
ejiri@meijo-u.ac.jp

Shoichi Fujimori
Department of Mathematics, Okayama University
Tsushimanaka, Okayama 700-8530, Japan.
fujimori@math.okayama-u.ac.jp

Toshihiro Shoda
Faculty of Culture and Education, Saga University
1 Honjo-cho, Saga-city, Saga, 840-8502, Japan.
tshoda@cc.saga-u.ac.jp